Femtosecond parabolic pulse nonlinear compression with gas-filled hollow-core fiber*

Huang Zhi-Yuan(黄志远)[a)b)], Leng Yu-Xin(冷雨欣)[b)†], and Dai Ye(戴 晔)[a)‡]

[a)] *Department of Physics, Shanghai University, Shanghai* 200444, *China*

[b)] *State Key Laboratory of High Field Laser Physics, Shanghai Institute of Optics and Fine Mechanics, Chinese Academy of Sciences, Shanghai* 201800, *China*

(Received 7 May 2014; revised manuscript received 11 June 2014; published online 10 October 2014)

We study theoretically the spectral intensity evolutions of the femtosecond Gaussian and parabolic pulses with different initial pulse energies and compare the nonlinear compressions of these pulses based on a meter-long hollow-core fiber filled with neon for different initial pulse durations. The pulses are first coupled into gas-filled hollow-core fiber for spectrum broadening, then compressed by the optimal chirp compensation. The parabolic pulse possesses a shorter pulse duration, larger peak power, and cleaner wings than Gaussian pulse. The properties are useful for compressing the pulses and thus generating the high-energy, short-duration pulses.

Keywords: parabolic pulse, nonlinear compression, hollow-core fiber, spectrum broadening

PACS: 42.65.Re, 42.65.Jx, 42.81.Qb **DOI:** 10.1088/1674-1056/23/12/124210

1. Introduction

Optical pulse compression through hollow-core fiber (HCF) has been developed into a powerful technique for generating intense few-cycle pulses in the visible and near-infrared spectral range.[1–4] Compared with the pulse compression using traditional optical fibers of bulk materials, the hollow-core fiber improves the output energy level to micro- and even milli-joule while preserving the few-cycle duration.[5] The basic principle of HCF compressor is simple. Intense pulses first propagate in a meter-long with gas-filled HCF to broaden the spectrum via self-phase modulation (SPM) and obtain positive chirp, then they are compressed by the suitable negative chirp compensation.[6–9] SPM effect plays a very important role in this process: it makes the pulse obtain the nonlinear phase related to pulse intensity in the time domain, and SPM-induced frequency chirp results from the time-dependent nonlinear phase shift. For a positively chirped pulse, when we compensate for the pulse in the anomalous dispersion region, the trailing edge moves faster than the leading edge. As a result, the pulse is compressed after an optimum propagation distance. It should be noted that only linear chirp produced in the spectral broadening process is useful for compressing the pulses. As is well known, Gaussian pulse is one of most widely used pulses. However, for Gaussian pulse, linear chirp generated in the nonlinear spectral broadening process concentrates mainly in a central portion of pulse. When we compensate for the pulse, only the central portion is compressed, and the pulse on both sides of the wing retains part of the energy not compressed, thus it is not a high-quality pulse.

Theoretical and experimental results showed that input optical pulses with parabolic temporal shapes are important for suppressing the undesired wave breaking in the nonlinear spectral broadening process, and contribute to a low-ripple supercontinuum generation and pulse compression compared with Gaussian pulse and other pulse shapes such as triangular pulse.[10,11] Parabolic pulse acquires a linear chirp after propagating in the HCF, then a high-quality pulse with shorter duration and cleaner wings is obtained by a suitable chirp compensation.[12] A few linear techniques including filtering with a specially-designed superstructured fiber Bragg gratings (SSFBG),[13] pulse shaping based on temporal coherence synthesization and long period fiber gratings (LPFGs) were used to obtain the different pulse shapes including parabolic pulse.[14,15] Moreover, the different pulse shapes are also developed by first using the amplifier to modify their spectrum and then being compressed by certain compensation.[16,17]

In this paper, we report on the first theoretical analysis of the femtosecond parabolic pulse nonlinear compression with gas-filled hollow-core fiber. The rest of this paper is organized as follows. In Section 2 the detailed model of nonlinear compression with gas-filled HCF is described. In Section 3, the differences in time and frequency domain between femtosecond Gaussian and parabolic pulses are compared, besides, SPM-induced frequency chirp produced from spectral

*Project supported by the National Natural Science Foundation of China (Grant Nos. 61221064, 61078037, 11127901, and 11134010), the National Basic Research Program of China (Grant No. 2011CB808101), the Funds from the Commission of Science and Technology of Shanghai, China (Grant No. 12dz1100700), the Natural Science Foundation of Shanghai, China (Grant No. 13ZR1414800), and the International S & T Cooperation Program of China (Grant No. 2011DFA11300).

†Corresponding author. E-mail: lengyuxin@siom.ac.cn

‡Corresponding author. E-mail: yedai@shu.edu.cn

© 2014 Chinese Physical Society and IOP Publishing Ltd

broadening process in the HCF is also analyzed in detail. Next, we simulate and compare the spectral evolutions of Gaussian and parabolic pulses with different initial energies that range from 0.1 mJ to 1 mJ for considering whether the effect of plasma appears. Then, several examples about spectral evolution for certain input pulse energy with increasing the distance of fiber and output pulses after compression by the optimum chirp compensation are given. Finally, we study numerically the Gaussian and parabolic pulse compressions by using the optimal group-delay dispersion (GDD) and third-order dispersion (TOD) compensations based on a meter-long hollow-core fiber filled with neon at different input pulse durations from ten to twenty cycles (central wavelength is 800 nm), in addition, we also show the compression ratio, peak power, and transmission versus different pulse cycles for these pulses. In Section 4 some conclusions are drawn from the present studies.

2. Model and methods

The spectrum broadening is achieved in a meter-long with gas-filled HCF based on self-phase modulation effect. Here, we use a single HCF with static gas pressure, and neon is used for a compromise between nonlinearity and ionization potential. The envelop $E(z,t,r)$, assumed to be slowly varying in time, evolves along the propagation axis z according to the fundamental mode equation,[18,19]

$$\frac{\partial E}{\partial z} = \mathrm{i}\hat{L}E + \mathrm{i}\hat{T}\left(\frac{\omega_0}{c}n_2\gamma|E|^2E\right) - \left[\frac{\sigma}{2}\mathrm{d}E + \frac{\mathrm{i}q_\mathrm{e}^2}{2c\omega_0 m_\mathrm{e}\varepsilon_0}\hat{T}^{-1}(\mathrm{d}E)\right] - \frac{f}{2|E|^2}E, \quad (1)$$

where linear operator

$$\hat{L} = \mathrm{i}\alpha^{(0)} - \alpha^{(1)}\partial/\partial_\tau + \sum_{m=2}^{\infty}(\mathrm{i}^m\partial^m/\partial_{\tau^m})[\beta^{(m)} + \mathrm{i}\alpha^{(m)}]/m!$$

describes the waveguide mode attenuation $\alpha^{(m)} = \mathrm{d}^m\alpha/\mathrm{d}\omega^m|\omega = \omega_0$ and dispersion parameter $\beta^{(m)} = \mathrm{d}^m\beta/\mathrm{d}\omega^m|\omega = \omega_0$ with the central angular frequency of the pulse ω_0. Here, τ refers to the retarded time variable $t - z/v_\mathrm{g}$ with group velocity $v_\mathrm{g} = 1/\beta^{(1)}$. Constants c, σ, q_e, m_e, and ε_0 are light speed in vacuum, impact ionization cross section, electron charge, and mass, and vacuum permittivity respectively. The operator $\hat{T} = 1 + (\mathrm{i}/\omega_0)(\partial/\partial_\tau)$ gives rise to self-steeping effects. n_2 denotes the nonlinear index of refraction proportional to the third order component $\chi^{(3)}$ of the susceptibility tensor of the gas. The coefficient $\gamma = \int_0^a V^4\cdot r\mathrm{d}r/\int_0^a V^2\cdot r\mathrm{d}r$ with pulse transverse mode $V = \mathrm{J}_0(ur/a)$, where r is the transverse coordinate, a is the fiber inner radius, $\mathrm{J}_0(x)$ is the 0th order Bessel function of the first kind, u is the first zero point of $\mathrm{J}_0(x)$; $d = \int_0^a \rho V^2\cdot r\mathrm{d}r/\int_0^a V^2\cdot r\mathrm{d}r$ with electron density ρ; $f = \int_0^a W(\rho_\mathrm{nt} - \rho)U_\mathrm{p}\cdot r\mathrm{d}r/\int_0^a V^2\cdot r\mathrm{d}r$, where W is the ionization rate, ρ_nt is the neutral density of the gas, and U_p is the ionization potential. The terms on the right-hand side of Eq. (1) describe the propagation losses and higher order dispersion, self-focusing related to the Kerr effect with self-steeping effect, defocusing due to the plasma, and energy absorption due to ionization respectively. Assuming electrons to be born at rest, the electron density evolves as

$$\frac{\partial\rho}{\partial t} = W(\rho_\mathrm{nt} - \rho) + \frac{\sigma}{U_\mathrm{p}}\rho|E|^2, \quad (2)$$

where ionization rate W is obtained by Perelomov, Popov, and Terent'ev (PPT) theory.[20]

The input parabolic pulse coupled into the fiber can be expressed as[14,18]

$$E(z=0,t,r) = \sqrt{I_\mathrm{peak}}\sqrt{1-2\frac{t^2}{T_\mathrm{p}^2}}\exp\left(-\frac{r^2}{w_0^2}\right) \quad (3)$$

at $|t| \le T_\mathrm{p}/\sqrt{2}$, where $E(z,t,r) = 0$ for $|t| > T_\mathrm{p}/\sqrt{2}$ and T_p is the pulse full width at half maximum (FWHM), I_peak denotes the pulse peak intensity, and the beam width w_0 is chosen to be $0.65a$ to guarantee that the energy coupled to fundamental mode is highest,[21] i.e. 98% of the total energy. The pulse energy is given by $U = 2\pi\iint|E|^2r\mathrm{d}t\,\mathrm{d}r$, then we can obtain the peak intensity I_peak, and according to input pulse energy U_0 it can be expressed as follows:

$$I_\mathrm{peak} = U_0/\left[\int_{-\infty}^{\infty}(1-2t^2/T_\mathrm{p}^2)\mathrm{d}t\int_0^{\infty}2\pi r\exp(-2r^2/w_0^2)\mathrm{d}r\right],$$

and further it can be written as $I_\mathrm{peak} = 3U_0/\sqrt{2}\pi w_0^2T_\mathrm{p}$ with considering the integral $\int_0^{\infty}r\exp(-2r^2)\mathrm{d}r = 0.25$.

3. Numerical results

The numerical values given in this section correspond to a central wavelength 800 nm of laser, the length of the HCF filled with neon gas is 1 m, the pressure within the fiber is set to be 1 bar (1 bar = 10^5 Pa), and the inner diameter is 250 μm.

We first compare the differences in time and frequency domain between femtosecond Gaussian and parabolic pulses. Figure 1(a) shows temporal profiles of pulses, and we can see that parabolic pulse has a higher peak power and steeper along the pulse front and back edge, while it has the opposite scenario to its spectral intensity from Fig. 1(b). These differences make Gaussian and parabolic pulses gain the different frequency chirps by SPM effect related to their pulses intensity. Figure 1(c) gives the SPM-induced frequency chirp in spectral broadening process in the HCF, and figure 1(d) shows the enlarged central part of Fig. 1(c). It is clear that parabolic pulse obtains linear frequency chirp for that process, while linear chirp mainly concentrates in the central portion of pulse for Gaussian pulse, and the former has a greater chirp value than the latter, thereby leading to different results in the nonlinear compression process.

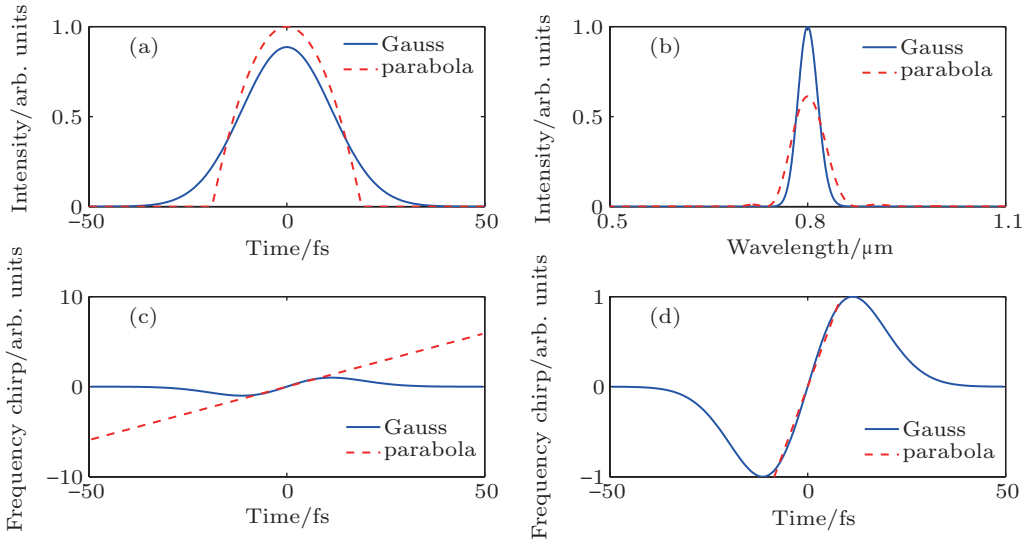


Fig. 1. (color online) Temporal profiles of Gaussian (solid curves) and parabolic (dashed curves) pulses (a), their spectral intensities (b), and SPM-induced frequency chirps (c). Panel (d) shows the enlarged central part of the curves in panel (c), with frequency chirp value ranging from −1 to 1.

Next, we compare and simulate the spectral intensity evolutions of Gaussian and parabolic pulses of 10 cycles (about 26.7 fs, FWHM) with different initial energies that range from 0.1 mJ to 1 mJ. Figures 2(a) and 2(b) show the spectral intensity evolutions of initial Gaussian and parabolic pulses, respectively. The latter has a wider spectrum, and the same scenario is shown in Fig. 1(b). In the case with considering the plasma effect, their output spectral evolutions are given in Figs. 2(c) and 2(d). We can see that Gaussian pulse presents a symmetric spectrum broadening with modulations from 0.4 mJ to 0.7 mJ, and a blue shift after 0.7 mJ.[22] For parabolic pulse, there is a symmetric spectrum broadening without modulations until 0.6 mJ after which a steady blue-shift is observed. Figures 2(e) and 2(f) show the results in the absence of plasma effect, in comparison with the middle row, it can be seen that these pulses exhibit only red shift and their spectral evolutions are more severe. In other words, plasma effect begins to play an important role after about 0.6 mJ, which leads to blue shift of spectral evolution. It should be noted that the spectrum modulation of Gaussian pulse is caused by spectral interference. Figure 1(d) shows that two different time points corresponds to the same frequency chirp value for the Gaussian pulse, while for the parabolic pulse only one time point corresponds to one frequency chip value.

Then, we study spectral evolution for a certain input pulse energy with increasing the distance of fiber for 10 pulse cycles. Figures 3(a) and 3(b) show the spectral evolutions of Gaussian and parabolic pulses in the HCF at an initial pulse energy of 0.4 mJ respectively. When the input energy is set to be 0.7 mJ, the simulation results are given in Figs. 3(c) and 3(d). For Gaussian pulse, the spectrum is split early and wide for the greater initial pulse energy. For parabolic pulse, its spectrum is blue-shifted and more intense than that of the Gaussian pulse.

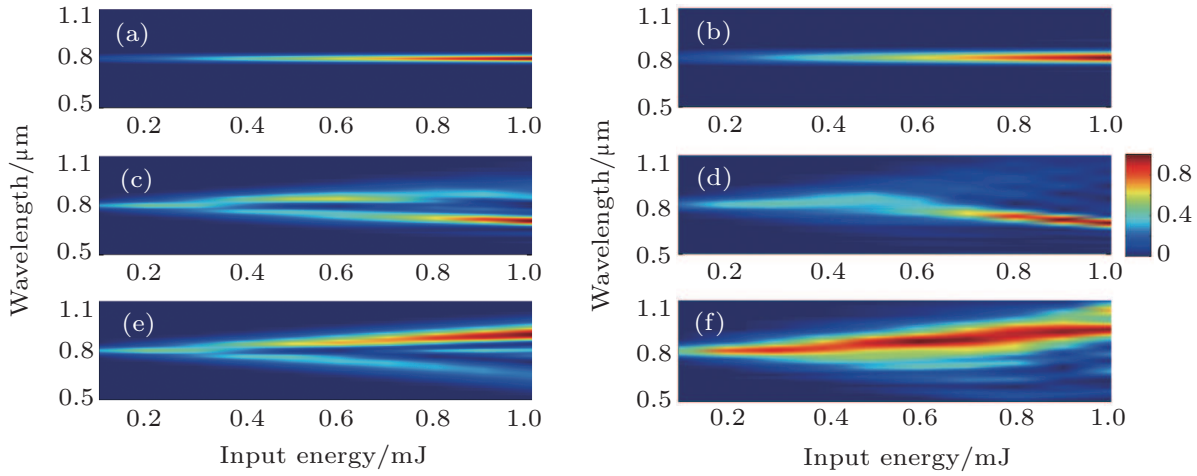


Fig. 2. (color online) Spectral intensity evolutions of Gaussian ((a), (c), and (e)) and parabolic ((b), (d), and (f)) pulses with initial energies ranging from 0.1 mJ to 1 mJ. Spectral evolutions of input pulses ((a) and (b)), output pulses with ((c) and (d)) and without ((e) and (f)) plasma effect.

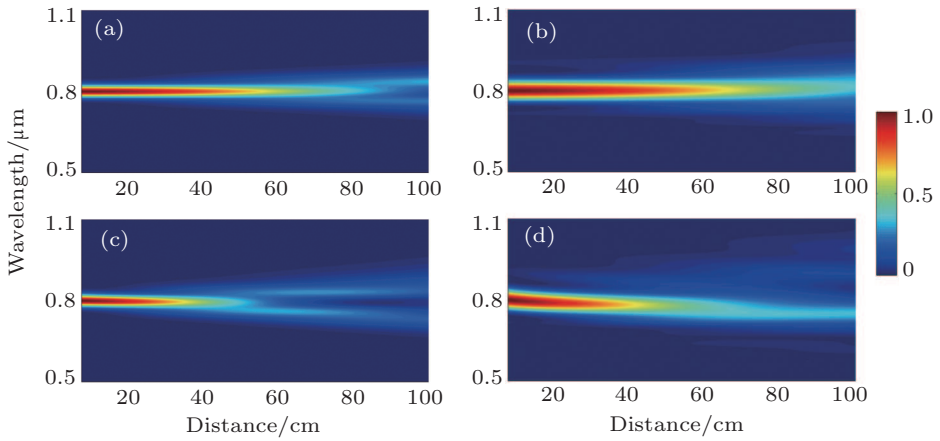


Fig. 3. (color online) Spectral intensity evolutions of Gaussian ((a) and (c)) and parabolic ((b) and (d)) pulses with the fiber distance increasing from 0 to 100 cm, where the first row corresponds to 0.4 mJ and the second row corresponds to 0.7 mJ.

Moreover, we simulate input Gaussian and parabolic pulses of 10 cycles (about 26.7 fs, FWHM) with different initial energies. Figures 4(a), 4(c), and 4(e) show the temporal intensity profiles of output pulses after compression with optimum chirp compensation at input energies of 0.1 mJ, 0.42 mJ, and 1 mJ, respectively, while figures 4(b), 4(d), and 4(f) show the temporal evolutions of their corresponding spectral intensities. We can see that the profiles and spectrum characteristics of output pulses in the second row (FWHM 8.1 fs for Gaussian pulse and 4.3 fs for parabolic pulse) are better than the other two rows (solid curves and dashed curves, 18.6 fs, 4.6 fs for Gaussian pulse and 10 fs, 3 fs for parabolic pulse, respectively). This is caused by initial pulse energy: for the small input energy, the nonlinear effects are weak which restricts the spectral broadening of pulse in the HCF, however, when the pulse intensity is quite high, the nonlinear effects become more obvious and they will cause the pulse to break up heavily. Here, initial pulse energy 0.42 mJ is the optimal for these three cases. Besides, it is clear that parabolic pulse obtains a shorter duration, a greater peak power and cleaner wings by a suitable chirp compensation, for which the main reason is that the parabolic pulse acquires a linear chirp after propagating in the HCF. In addition, for the greater initial pulse energy (such as Fig. 4(e)), the peak power of parabolic pulse is smaller than that of Gaussian pulse: this phenomenon may be caused by the plasma effect.

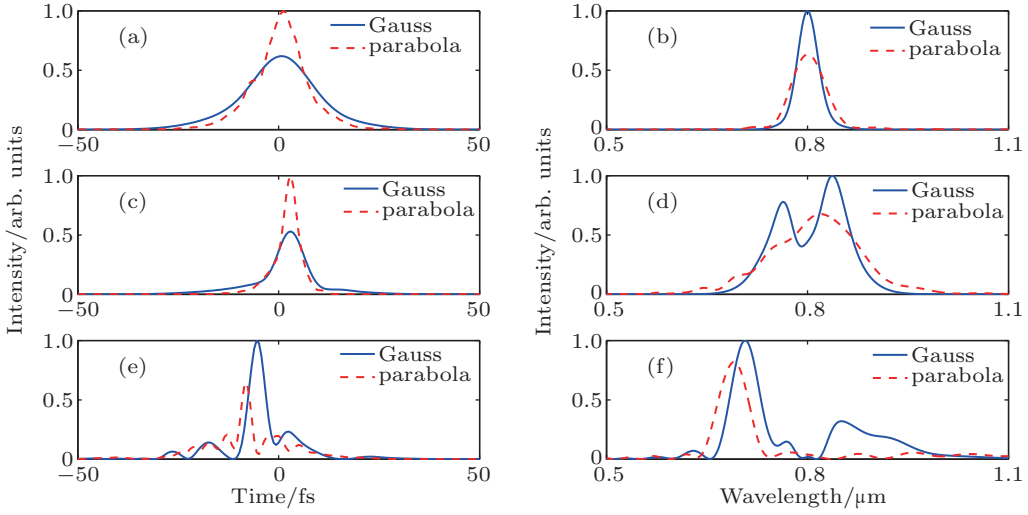


Fig. 4. (color online) Temporal profiles of Gaussian (solid curves) and parabolic (dashed curves) output pulses ((a), (c), and (e)) and their spectral intensities ((b), (d), and (f)) after compression with optimal chirp compensation for initial energies of 0.1 mJ, 0.42 mJ, 1 mJ respectively.

Finally, we consider the evolutions of Gaussian and parabolic input pulses with pulse durations that range from ten cycles (about 26.7 fs, FWHM) to twenty cycles (about 53.3 fs, FWHM) at initial energy 0.42 mJ. Figures 5(a) and 5(b) show the temporal intensities of Gaussian and parabolic pulses after chirp compensation with increasing the input cycle respectively. It is obvious that the parabolic pulse obtains a shorter pulse duration and cleaner wings than the Gaussian input pulses under the same conditions but different input cycles. The values of compression ratio (input pulse duration to output pulse duration) and

peak power of these pulses are shown in Figs. 5(c) and 5(d), respectively. We notice that parabolic pulses have excellent results in both compression ratio and peak power. Figure 5(e) shows the transmittances of the pulses for different input cycles. We can see that Gaussian pulse transmittances are slightly larger and their values range from 0.86 to 0.87 at different pulse durations.

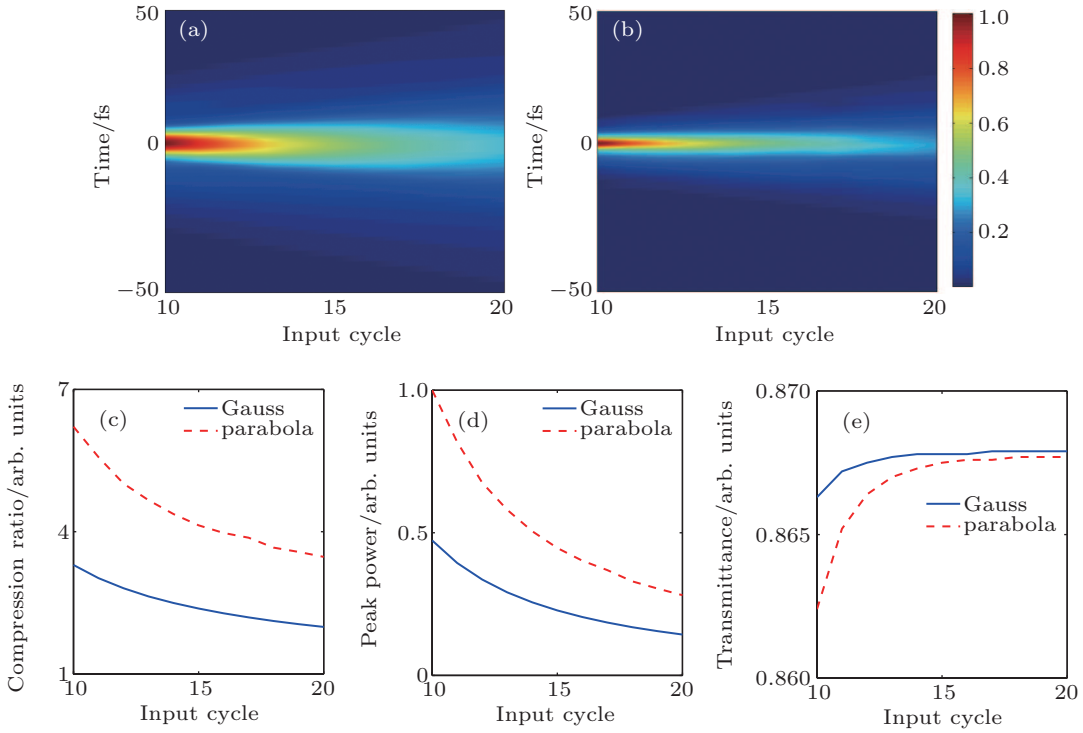


Fig. 5. (color online) Intensity variations of Gaussian (solid curves) (a) and parabolic (dashed curves) (b) pulses after chirp compensation, and their compression ratios (c), peak powers (d), and transmittances (e) with input cycle at initial energy 0.42 mJ.

4. Conclusions

In this paper, we compare and simulate the spectral intensity evolutions of Gaussian and parabolic pulses of 10 cycles with initial energies ranging from 0.1 mJ to 1 mJ based on a meter-long hollow-core fiber filled with neon and study theoretically the nonlinear compressions of Gaussian and parabolic pulses by using the optimal chirp compensation for different initial pulse durations from ten to twenty cycles. Moreover, we also analyze the SPM-induced frequency chirp produced in the spectral broadening processes of Gaussian and parabolic pulses. For Gaussian pulse, linear chirp concentrates mainly in the central portion of pulse, while for parabolic pulse, it obtains a linear chirp. This difference causes many different and interesting results in the nonlinear compression process. Our results clearly show that the parabolic pulse possesses a shorter pulse durations, larger peak power, and cleaner wings than Gaussian pulse under the same conditions. These results could be used to compress ultrafast pulses with higher energies and shorter durations.

References

[1] Wang F, Jiang H B and Gong Q H 2014 *Chin. Phys. B* **23** 014201
[2] Nisoli M, Silvestri S D and Svelto O 1996 *Appl. Phys. Lett.* **68** 2793
[3] Mashiko H, Nakamura C M, Li C, Moon E, Wang H, Tackett J and Chang Z 2007 *Appl. Phys. Lett.* **90** 161114
[4] Mansour B F and Anis H 2006 *Opt. Lett.* **31** 3185
[5] Wang D, Leng Y X and Xu Z Z 2012 *Opt. Commun.* **285** 2418
[6] Chen X W, Zeng Z N, Dai J, Li X F, Li R X and Xu Z Z 2008 *Chin. Phys. B* **17** 1826
[7] Kang Z, Yuan J H, Li S, Xie S L, Yan B B, Sang X Z and Yu C X 2013 *Chin. Phys. B* **22** 114211
[8] Chen H W, Guo L, Jian A J, Chen S P, Hou J and Lu Q S 2013 *Acta Phys. Sin.* **62** 154207 (in Chinese)
[9] Liu S L, Chen D N, Liu W and Niu H B 2013 *Acta Phys. Sin.* **62** 184210 (in Chinese)
[10] Krmačmařík D, Slavík R, Park Y and Azaña J 2009 *Opt. Express* **17** 7074
[11] Anderson D, Desaix M, Karlsson M, Lisak M and Quiroga-Teixeiro M L 1993 *J. Opt. Soc. Am. B* **10** 1185
[12] Andresen E R, Dudley J M, Oron D, Finot C and Rigneault H 2011 *Opt. Lett.* **36** 707
[13] Parmigiani F, Finot C, Mukasa K, Ibsen M, Roelens M A F, Petropoulos P and Richardson D J 2006 *Opt. Express* **14** 7617
[14] Park Y, Asghari M H, Ahn T J and Azaña J 2007 *Opt. Express* **15** 9584
[15] Slavík R, Park Y and Azaña J 2008 *Photon. Technol. Lett.* **20** 806
[16] Kruglov V I, Thomsen B C, Dudley J M and Harvey J D 2000 *Phys. Rev. Lett.* **84** 6010
[17] Zhao J S, Li P, Chen X D, Feng S J and Mao Q H 2012 *Chin. Phys. B* **21** 094217
[18] Courtois C, Couairon A, Cros B, Marques J R and Matthieussent G 2001 *Physics of Plasmas* **8** 3445
[19] Wang D, Leng Y X and Huang Z Y 2014 *J. Opt. Soc. Am. B* **31** 1248
[20] Bergé L, Skupin S, Nuter R, Kasparian J and Wolf J P 2007 *Rep. Prog. Phys.* **70** 1633
[21] Dorchies F, Marquès J R, Cros B, Matthieussent G, Courtois C, Vélikoroussov T, Audebert P, Geindre J P, Rebibo S, Hamoniaux G and Amiranoff F 1999 *Phys. Rev. Lett.* **82** 4655
[22] Babin A A, Kartashov D V, Kiselev A M, Lozhkarev V V, Stepanov A N and Sergeev A M 2002 *Appl. Phys. B* **75** 509